Engineering Failure Analysis 138 (2022) 106409

Contents lists available at ScienceDirect

Engineering Failure Analysis

journal homepage: www.elsevier.com/locate/engfailanal

Analysis of thrust blocks systems: Pipeline, soil and foundation interaction

Josefina Barrera [a], Franco Carpio [b,*], Alberto Jaime [a], Fernando Peña [a], Alejandro Sánchez [a]

[a] *Instituto de Ingeniería, Universidad Nacional Autónoma de México, Circuito Escolar, Ciudad Universitaria, C.P. 04510, Mexico City, Mexico*
[b] *Instituto de Ingeniería, Universidad Veracruzana, Av. Juan Pablo II S/N, Zona Universitaria, C.P. 94294, Boca del Río, Veracruz, Mexico*

A R T I C L E I N F O

Keywords:
Thrust blocks
Numerical modelling
Structural behavior
Soil-thrust block-pipeline interaction
High pressure pipeline

A B S T R A C T

The aim of this study is to evaluate the behavior of a discharge manifold that has space restrictions. These restrictions do not allow a suitable design by the usual practice. Thus, for its evaluation an upgraded methodology was necessary for structural analysis and revision. The upgrade includes the soil-thrust blocks-pipeline interaction and the influence of fittings outside the blocks using a simplified model. The manifold was assumed as a whole structure. The pipeline was modelled with frame elements. The behavior of the thrust blocks was simulated by means of a Winkler-like model with torsional and horizontal springs. Additionally, the influence of reducers and valves lying outside the blocks was included. Two analyses were performed. The first one, the interaction between soil, thrust blocks and pipeline is neglected; the second one includes the interaction among the elements. It is concluded that the overall capacity of the structural system increases when the interaction among elements is considered. The effects due to the interaction and the fittings lying outside the blocks can be estimated with the proposed model. Finally, it is shown that the reducers not embedded in the blocks produce a significant increment (up to 47%) in the pipeline longitudinal stresses. Nevertheless, the manifold resulted suitable for its operation. Thus, to evaluate a manifold that has space restrictions the enhanced methodology described in this paper can be used.

1. Introduction

1.1. Background

Many water systems require pumping stations (Fig. 1a). In these cases, the structural steel pipe is recommended, due to its capacity to withstand internal and external pressure, bending and its durability. According to the project needs, some fittings are installed in the pipeline, such as: bends, valves, and reducers or conical transitions. Fittings add forces on the pipeline that must be considered in the design. Other actions on the pipeline are those caused by changes in vertical and horizontal direction of the water flow. Thrust blocks are reinforced concrete structures that withstand these forces and constrain the pipe displacements (Fig. 1b). Similarly, the pump bases withstand the forces and constrain the displacements (Fig. 1c).

* Corresponding author.
E-mail addresses: jbarrerag@iingen.unam.mx (J. Barrera), fcarpio@uv.mx (F. Carpio), ajaimep@iingen.unam.mx (A. Jaime), fpem@pumas.iingen.unam.mx (F. Peña), asanchezh@iingen.unam.mx (A. Sánchez).

https://doi.org/10.1016/j.engfailanal.2022.106409
Received 9 September 2021; Received in revised form 22 March 2022; Accepted 5 May 2022
Available online 10 May 2022

Fig. 1. Pumping station: a) Aerial view of a pumping station, pipeline, and standpipe; b) Thrust blocks in a manifold; and c) Pumps and their bases.

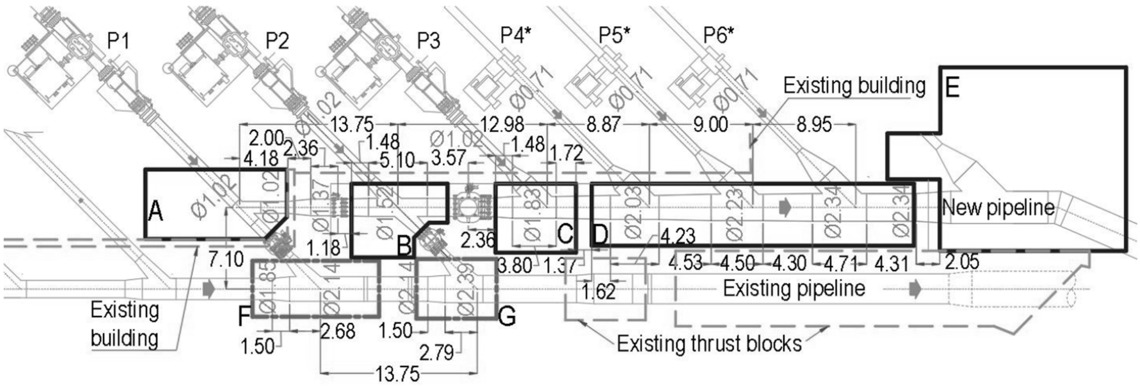

Fig. 2. Model arrangement of the discharge manifolds.

In many cases, the water systems require upgrades and expansions due to increments in demand or maintenance needs. For example, Bushdiecker *et al.* [1] wrote about the redevelopment of a water operations complex that involved pipe and thrust blocks relocations. They dealt with difficult site constraints and evaluated several thrust restraint alternatives. The analysis did not involve a model of the system and the pipes were buried. Jeyapalan and Rajah [2] investigated the pipe movements during pressure tests of two water lines; a tridimensional finite element analysis was performed in which the pipelines, the pump station piping, and the fittings were modeled. The pipelines were buried, and it was studied the influence of the thrust blocks and/or expansion joints in the system to prevent further movements.

In the present paper, a case of a pumping station, whose main pipeline is not buried and has operated with one main pipeline is described. The plan view of the discharge manifold is shown in Fig. 2 (dimensions in m, external diameters provided). Currently, some pumps in this manifold need maintenance but, to maintain the volume flow rate, it has been delayed. Therefore, it was decided to add a new mainline and reconfigure the manifold so that the volume flow rate through the existing pipeline would be up to 20 m^3/s and through the new pipeline up to 17.1 m^3/s.

The existing main pipeline would receive the volume of five 4.0 m^3/s pumps, while the new pipeline would receive the volume of three 4.0 m^3/s pumps and three 1.7 m^3/s pumps. The reconfiguration considers that two 4.0 m^3/s pumps are connected to the two main pipelines (Fig. 2). The reconfigured pump station will have two discharge manifolds and two independent pipelines. Each pipeline has several thrust blocks, valves and fittings that lie close to each other. In this scenario, the stiffness of the pipelines is significant in the overall behavior of the system as it will be shown in the results of the analysis taking into account the structural interaction.

Installing a new parallel pipeline and adapting the pump station have many difficulties. In this case, there were two buildings, existing thrust blocks and the pumps were already installed and in operation. The block A of the new pipeline must be constructed in the basement of an existing building (dashed line, Fig. 2); therefore, the height is restricted by the floor ceiling. Blocks B, C and D have to be built in the space between a building and the existing thrust blocks. Moreover, reducers and valves must be installed considering these constraints.

There are some studies about water pipelines and water supply systems. Kuliczkowska *et al.* [3] studied the structural integrity of water pipelines. The results of the case study indicate to what extent different loads influence the amount of stress in a pipeline. Depending on the assumptions made, the total stresses in the pipeline can vary up to several times. Pietrucha-Urbanik [4] performed a failure analysis of water supply failure frequency in one of the biggest cities in Poland. The analysis of water pipes failures was made including various pipes diameters, their age, and their function in the water supply subsystem in the city.

For the pipeline, the common analysis is focused on long length pipe segments. Thus, the effects produced by the thrust blocks and fittings are not considered. While, for the thrust blocks design, each structure is considered as an independent unit, neglecting the pipe resistance [5,6]. Hence, the soil-thrust block-pipeline interaction is not considered in the recommended manual design.

Some studies have analyzed the soil-pipeline interaction. ASCE [7] studied the friction and passive contribution to thrust resistance in buried pipes. This committee [8] provided a framework for the design of a thrust block for a horizontal bend in buried pipelines, considering the allowable movement of the pipe. Rajah *et al.* [9] studied the soil structure interaction effects in thrust restraint systems of buried pipelines. They modelled steel pipe bends and performed finite element analyses. Zangh *et al.* [10] used the unit force method to analyze thrust acting on anchor blocks that restrict the thermal expansion displacement of tunnel pipelines. A simplified mechanical model and finite element analyses were performed. Bardakjan and Zarghamee [11] studied a 120 in diameter steel bifurcation for a high pressure penstock using finite element analyses.

Furthermore, most manuals and codes [12,13] that deal with high pressure pipeline projects are intended mainly for buried pipelines. Hence, these provide scant guidance about analysis and design of thrust blocks for supported pipelines. With regards to the seismic analysis, Karamanos *et al.* [14] studied the seismic action on buried steel water pipelines with analytical methods and with finite element analysis, only the ASCE [5] provides some guidance about this revision in aboveground thrust blocks.

For the analysis and design of supported pipelines, the codes and manuals assume that the thrust blocks do not move, they are considered as fixed supports [6]. Therefore, in the case of the hydrostatic actions, the pipeline must only withstand radial stresses, and the Poisson effect in its longitudinal axis. The design requirements of thrust blocks include the revision of sliding and overturning effects. Likewise, the manuals consider that, except for the valves, the fittings (bends, wyes, reducers, etc.) must be embedded inside the thrust blocks. Matta and Dotson [15] analyzed unburied pipeline spans and their support requirements using theoretical evaluations and finite element analyses. Analyses of supported pipelines and thrust blocks as part of a pumping station, considering the soil-thrust blocks-pipeline interaction, were not found in the literature. Therefore, to study a case that has space restrictions that do not allow a suitable design by usual manual methods; thus, it was necessary to propose an enhanced methodology. For example, the soil-thrust blocks-pipeline and not encased fittings can be included using a numerical model [5]. In this model, the manifold is assumed to behave as a whole structure. Therefore, it is possible to calculate the redistribution of mechanical elements due to the interaction. To that effect, a practical approach to include the soil-thrust blocks-pipe line interaction is proposed in this paper.

1.2. Objective

The main objective of this paper is to evaluate the behavior of a discharge manifold having space restrictions, such as existing installations (connecting new and old thrust blocks) and buildings that do not allow a common practice design. To that end, the common method to perform the structural analysis and design was upgraded. Thus, for its evaluation, the soil-thrust blocks-pipeline interaction and the influence of fittings outside the blocks were considered. To estimate its structural behavior, a simplified (frame and spring) model is developed that incorporates the interaction and the influence of fittings not encased in the blocks.

1.3. Scope

Thus, in this paper, the interaction among soil, thrust blocks and the supported pipeline in a real case study is evaluated (Fig. 2). Two scenarios were considered. The first one, as suggested by the manuals, the interaction among thrust blocks and pipeline is neglected. The second takes into account the interaction among the different components by means of a simplified numerical model in order to evaluate their displacements and redistribution of mechanical elements.

The simplified numerical model considers the response of the blocks, due to soil-structure interaction, and the stiffness of the pipeline, supports, and fittings outside the blocks are considered. From the results of the numerical model, the structural interaction effects among the blocks and the pipe were analyzed, as well as the effects of having some of the reducers not embedded in the blocks. Finally, the structural behaviors of the manifold including these additional effects and without them are compared.

2. Common structural analysis and design

Technical manuals on steel pipelines consider the structural elements (pipes and thrust blocks) to behave independently, therefore the interaction between these elements is neglected. However, when the facility has many structures close to each other, many hypotheses that are considered in the most usual design methods are not fulfilled.

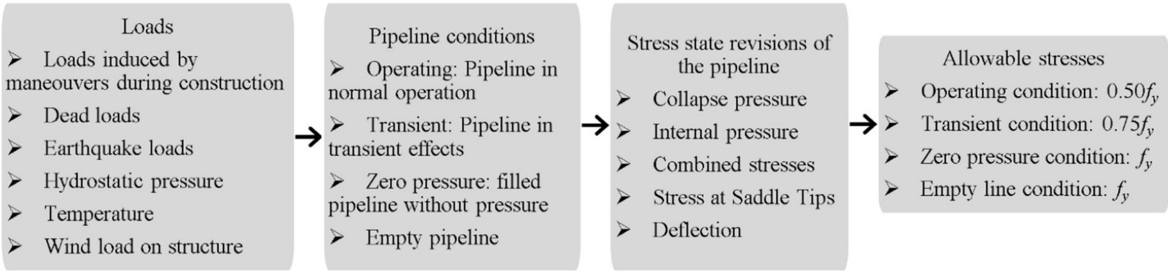

Fig. 3. Steps in the analysis and design of steel supported pipelines according to AWWA [12].

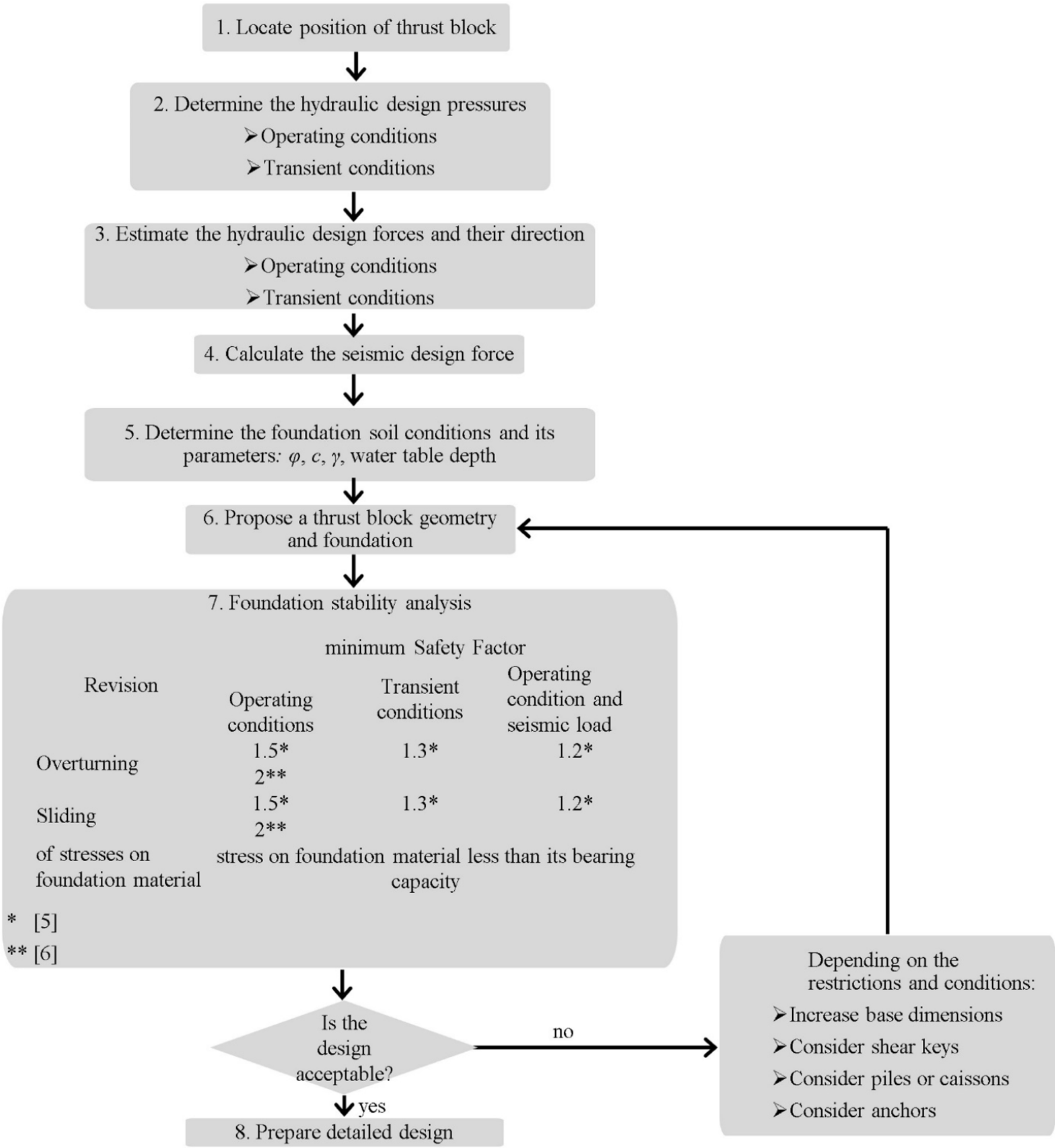

Fig. 4. Steps in the analysis and design of thrust blocks.

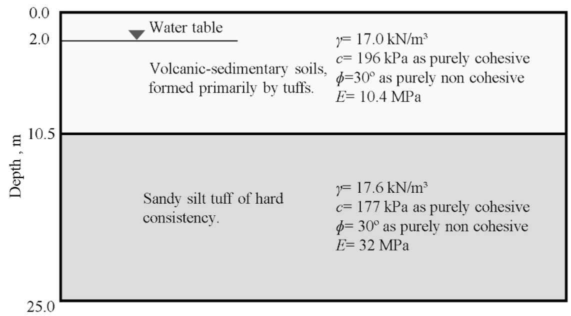

Fig. 5. Idealized soil stratigraphic profile.

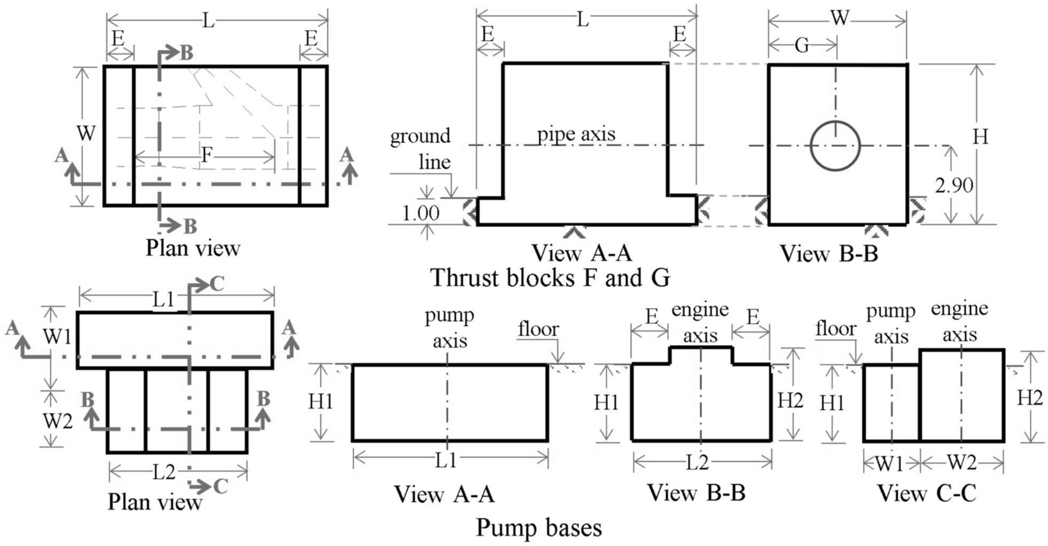

Fig. 6. Geometry description of existing thrust blocks and pump bases.

Table 1
Dimensions of existing thrust blocks and pump bases. Thrust blocks in the existing pipeline (F and G).

Thrust block	Dimension					
	L (m)	W (m)	H (m)	E (m)	F (m)	G (m)
F	11.00	4.85	5.70	1.50	4.40	2.43
G	7.00	5.20	5.90	1.00	4.30	2.60
Pump base	**Dimension**						
	L1 (m)	**L2 (m)**	**W1 (m)**	**W2 (m)**	**H1 (m)**	**H2 (m)**	**E (m)**
P1, P2, P3	12.00	8.00	3.00	4.00	2.00	3.30	2.50
P4*, P5*, P6*	7.00	5.00	2.00	3.00	2.65	3.30	1.40

See Fig. 6.

2.1. Pipeline

The design of steel supported pipelines [12,6] takes into account the load effects during different conditions as: normal operation, maintenance and transient effects (Fig. 3). The corrosion is considered by a reduction of the pipe thickness. This reduction is applied to the geometrical properties.

For the design of supported pipelines, several combinations of stress state are taken into account. Each stress state has different allowable stresses (Fig. 3), which are lower than the yield stress of the pipeline steel (f_y). In a first step, it is defined a pipe thickness to

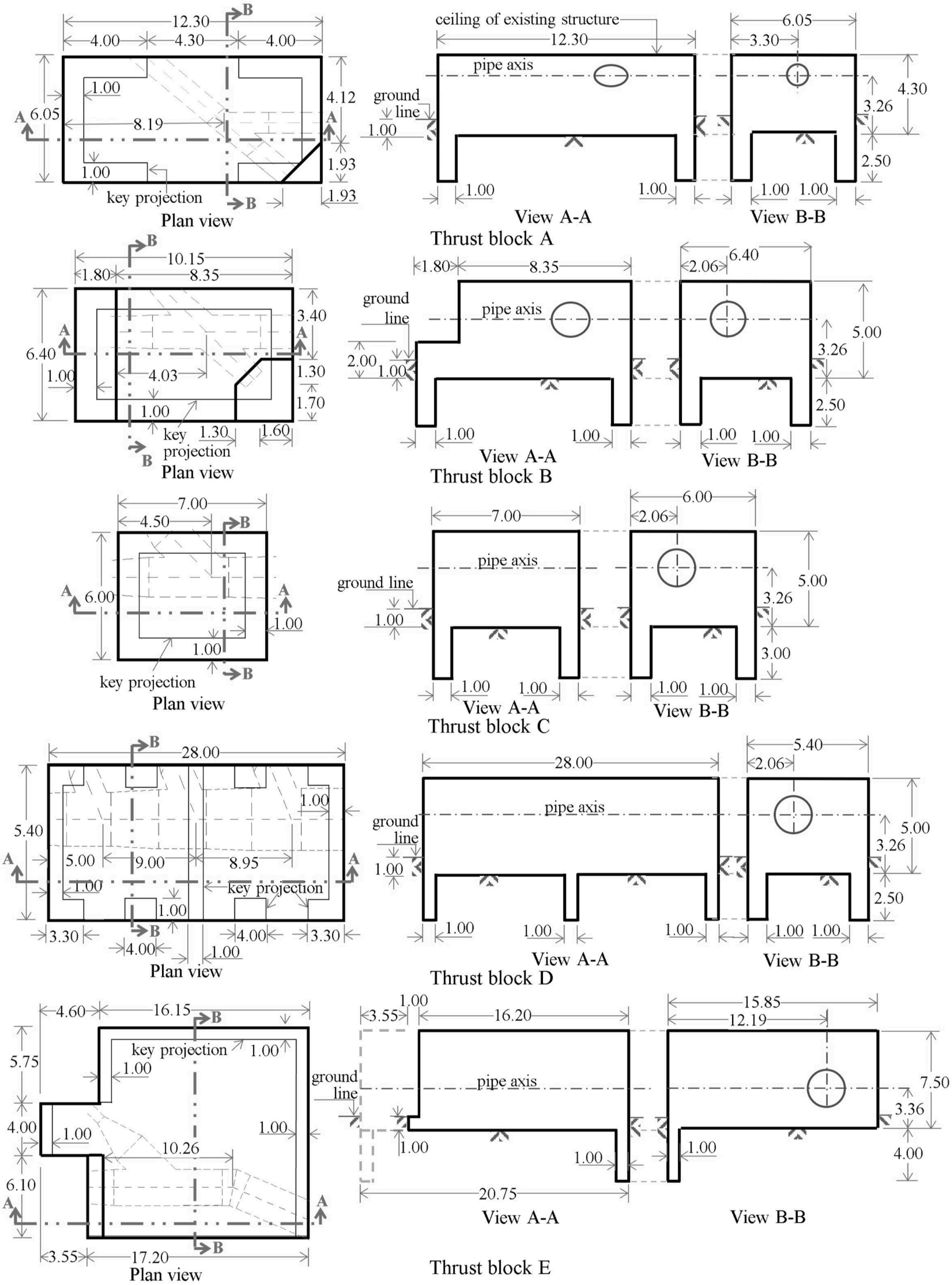

Fig. 7. Geometry description of new thrust blocks, dimensions in meters.

withstand the radial pressures produced by hydrostatic pressure along the pipeline. In a second step, the longitudinal stress is estimated with radial pressures along the pipeline path. Both principal stresses are considered to calculate the von Misses stress. To evaluate the combined stress, the von Misses stress and the allowable stress are compared.

In the studied discharge manifold (Fig. 2), the unsupported pipeline segments are short. Therefore, its structural design is defined by the internal pressure and the combined stress. In contrast, the deflections, the stress at the saddle tips and collapse pressure are insignificant.

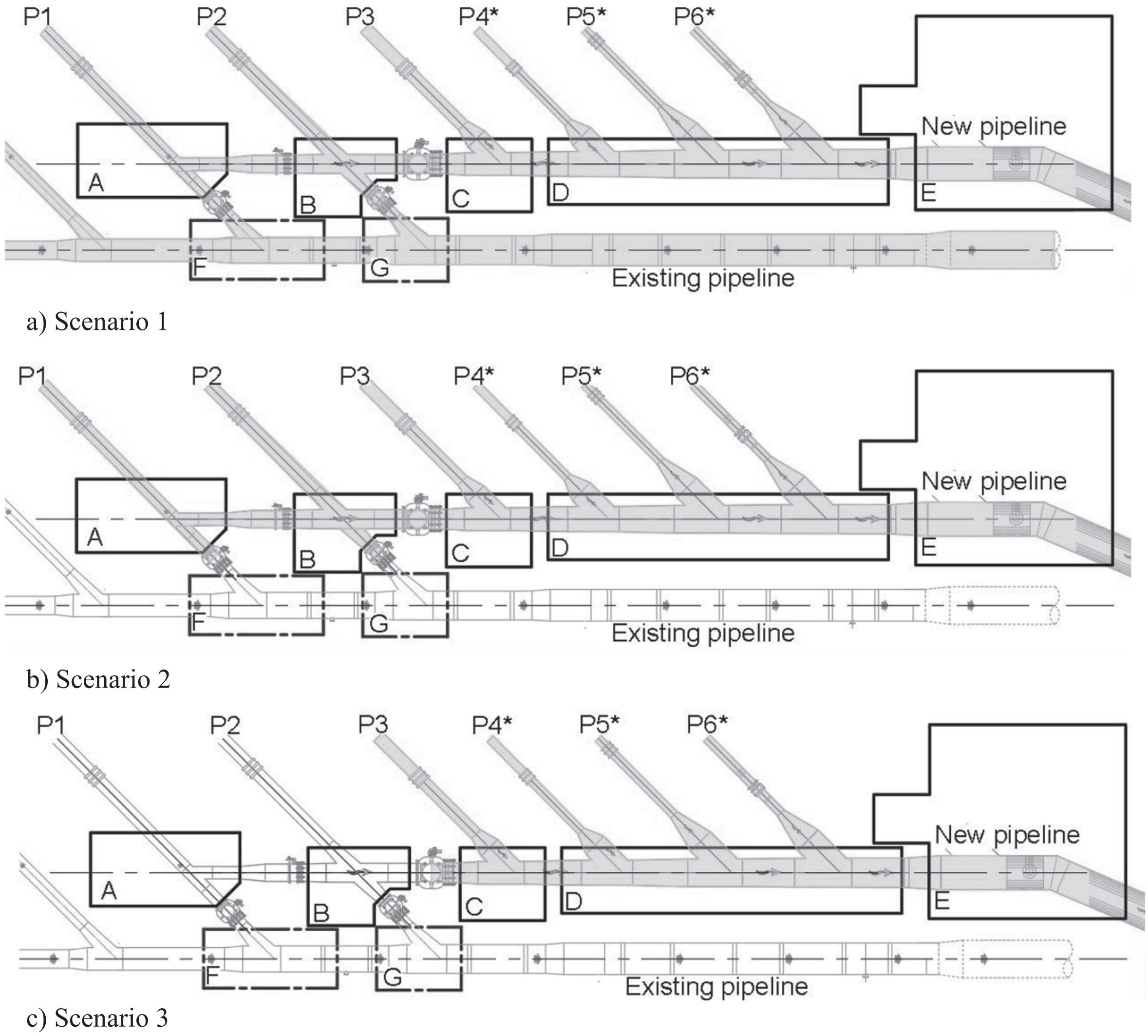

Fig. 8. Operating working scenarios a) 1, b) 2 and c) 3.

2.2. *Thrust blocks*

Thrust blocks design guidelines focus mainly on buried pipelines and take into account a significant passive soil resistance (*e. g.* AWWA [12]). It is well known that, to develop the passive resistance, the foundation must displace significantly (several centimeters) [16]. For this reason, the design guidelines recommend taking only part of the passive soil resistance, because large movements can affect the pipe and its fittings. On the other hand, friction resistance of soils fully develops at much lower displacements than the passive resistance. This soil friction response is of significant magnitude.

A common design process of thrust blocks is shown in Fig. 4, taking into account the work of Thorley and Atkinson [13], MAPAS 6 [6] and ASCE [5]. These recommendations do not include the torsional evaluation. The usual design guidelines assume that the encased pipeline and fittings are strong enough to resist the bending and shear stresses and the movement at the reducers is fully restricted.

Some manuals (*e.g.* MAPAS 6 [6]) include provisions for supported pipelines. For these cases, it states that if the pipeline has bends and reducers, it is required to have thrust blocks for resisting the forces that are generated by the changes in direction, both horizontal and vertical. The thrust blocks work as fixed supports that restrain all possible motions. These manuals also consider the possibility of using anchors for increasing the overturning resistance and decreasing the block size. The analysis must be made with the most unfavorable conditions and load combinations, including the effects of fittings, such as valves, bends, reducers, etc.

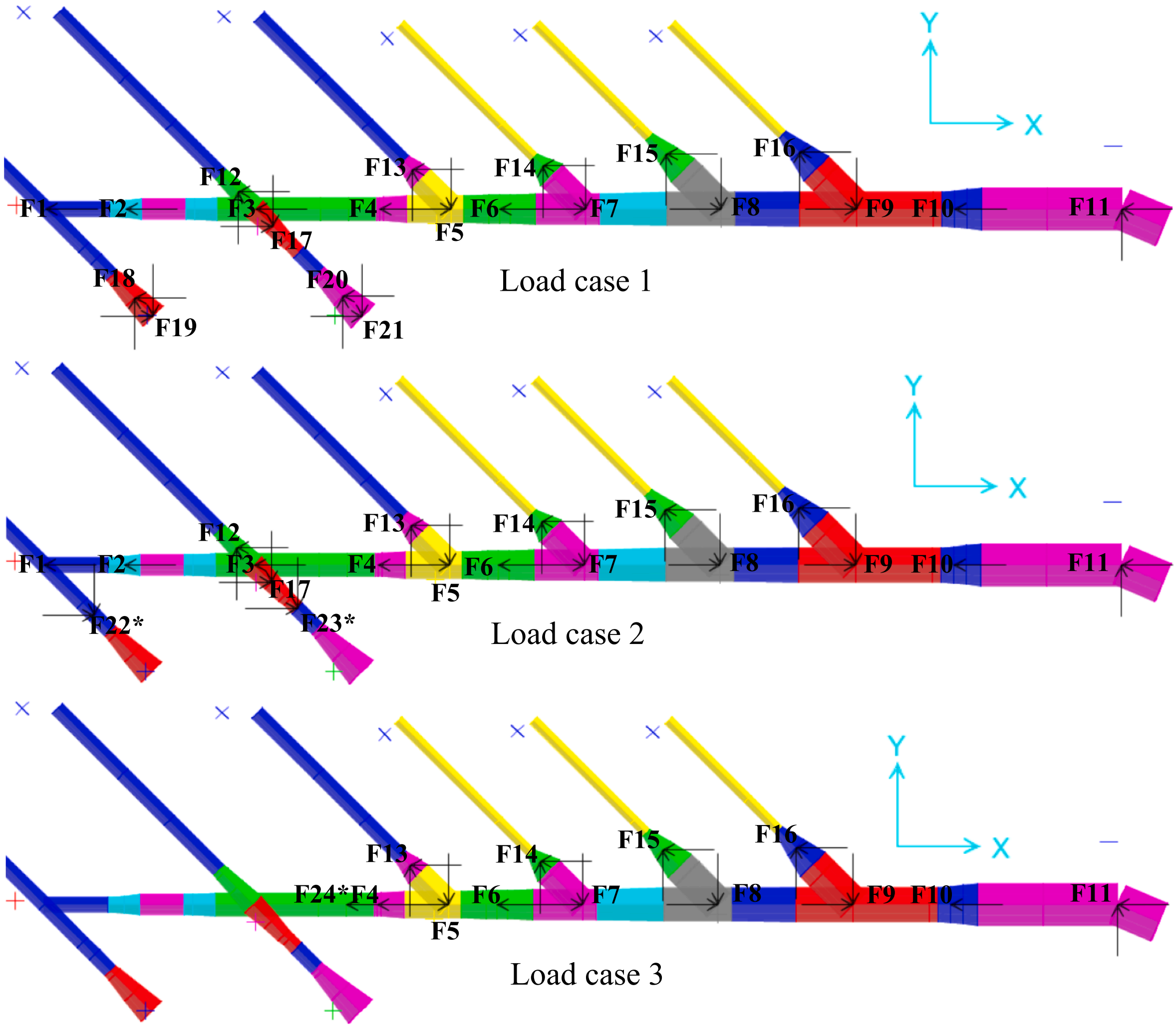

Fig. 9. Forces acting on each member of the model.

3. Description of the case study

3.1. Arrangement of the discharge manifolds

The discharge manifold of the new pipeline involves thrust blocks A, B, C, D and E. The pipeline changes direction at block E (Fig. 2). The new pipeline and the existing one connect at the F and G thrust blocks. These thrust blocks were considered in the studied cases. Likewise, the position of the pumps and their bases was included in the analysis. The P1, P2 and P3 pumps have a 4.0 m^3/s volume flow rate capacity, each one; the P4*, P5* and P6* pumps have a 1.7 m^3/s capacity, each one.

3.2. Soil properties

The stratigraphic profile of the site consists of volcanic-sedimentary soils, formed primarily by tuffs, such as depicted in Fig. 5. The material is brown with yellow and red undertones, with interspersed fragments of 3 to 15 cm in diameter. The shallow tuffs (10.5 m thick) show a sandy silt matrix mainly, and, in some areas, these are clayey or silty clayey. The water level is located at 2 m depth.

The soils index and mechanical properties were determined with samples from two borings. Besides, two plate load tests were performed at 2 and 3 m depth. From undrained unconsolidated triaxial tests, the material of the uppermost layer can be considered as either cohesive or non cohesive. In the first case, it was assumed a cohesion c of 196 kPa, in the second, the friction angle ϕ is equal to 30°. From the tests, the elastic modulus E was determined as 10.4 MPa. The unit weight of the soil γ_s is equal to 17 kN/m^3. For the deeper layer it was assumed a cohesion c of 177 kPa as purely cohesive, a friction angle ϕ of 30° as purely non cohesive. From the tests, the elastic modulus E was determined as 32 MPa. The unit weight of the soil γ_s is equal to 17.6 kN/m^3.

Table 2
Forces induced by the three load cases (kN).

Load		Case		
		1	2	3
F1	X=	−1471	−1471	closed
	Y=	0	0	closed
F2	X=	−1314	−1314	closed
F3	Y=	0	0	closed
	Y=	0	0	closed
F4	X=	−579	−579	−579
	Y=	0	0	0
F5	X=	1863	1863	1863
	Y=	−3619	−3619	−3619
F6	X=	−373	−373	−373
	Y=	0	0	0
F7	X=	4354	4354	4354
	Y=	−4492	−4492	−4492
F8	X=	4090	4090	4090
	Y=	−5453	−5453	−5453
F9	X=	5237	5237	5237
	Y=	−4992	−4992	−4992
F10	X=	−2569	−2569	−2569
	Y=	0	0	0
F11	X=	−108	−108	−108
	Y=	4805	4805	4805
F12	X=	−726	−726	closed
	Y=	726	726	closed
F13	X=	−2550	−2550	−2550
	Y=	2550	2550	2550
F14	X=	−3991	−3991	−3991
	Y=	3991	3991	3991
F15	X=	−4962	−4962	−4962
	Y=	4962	4962	4962
F16	X=	−5482	−5482	−5482
	Y=	5482	5482	5482
F17	X=	726	726	closed
	Y=	−726	−726	closed
F18	X=	−951	closed	closed
	Y=	951	closed	closed
F19	X=	226	closed	closed
	Y=	−2020	closed	closed
F20	X=	−1128	closed	closed
	Y=	1128	closed	closed
F21	X=	422	closed	closed
	Y=	−2207	closed	closed
F22*	X=	0	1069	closed
	Y=	0	−1069	closed
F23*	X=	0	1069	closed
	Y=	0	−1069	closed
F24*	X=	0	0	−3512
	Y=	0	0	0

Closed: line segment with no operation by closed valve.
*: closed valve.

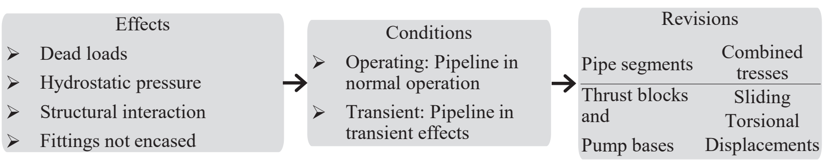

Fig. 10. Revision consideration to the study case.

3.3. Pipelines geometry and properties

The pipe has a nominal thickness t of 25.4 mm and is made of steel A53 Grade B with a yield strength f_y of 240 MPa and a modulus of elasticity E of 200,000 MPa. To take into account the corrosion effect to 50 years of life span, the pipe's thickness was reduced 1.30 mm

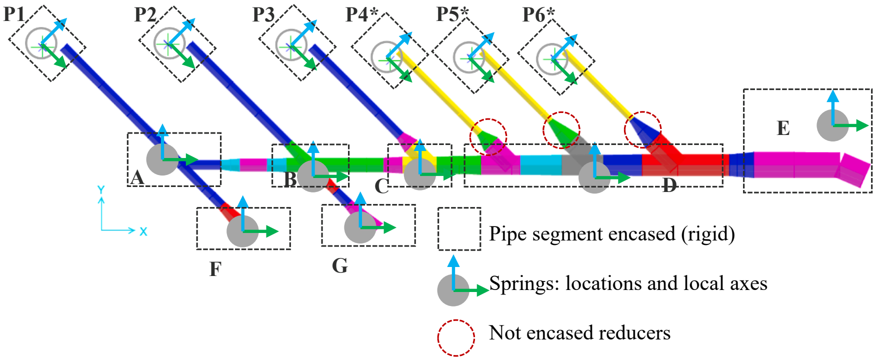

Fig. 11. Numerical model.

Table 3
Torsional stiffnesses of foundations.

Foundation	Translational stiffness		Polar moment of inertia	Rotational stiffness (Z)
	Longitudinal	Transversal		
	(kN/m)	(kN/m)	(m^4)	(kN-m/rad)
A	$1.28x10^{07}$	$9.59x10^{07}$	$1.17x10^{03}$	$3.09x10^{07}$
B	$1.36x10^{07}$	$4.94x10^{07}$	$8.47x10^{02}$	$2.25x10^{07}$
C	$1.14x10^{07}$	$1.75x10^{07}$	$2.98x10^{02}$	$7.88x10^{06}$
D	$9.40x10^{06}$	$1.67x10^{08}$	$1.03x10^{04}$	$2.72x10^{08}$
E	$1.20x10^{07}$	$1.54x10^{08}$	$1.33x10^{04}$	$3.51x10^{08}$
F	$1.78x10^{07}$	$1.41x10^{08}$	$6.43x10^{02}$	$1.70x10^{07}$
G	$2.76x10^{08}$	$7.84x10^{07}$	$2.31x10^{02}$	$6.11x10^{06}$
Big pump base	$4.15x10^{07}$	$1.48x10^{08}$	$7.53x10^{02}$	$1.99x10^{07}$
Small pump base	$1.14x10^{07}$	$2.43x10^{07}$	$1.23x10^{02}$	$3.26x10^{06}$

Table 4
Sliding and torsional resistance of foundations.

Foundation	Resistance		
	Longitudinal sliding (kN)	transversal sliding (kN)	Torsional (kN-m)
A	1971	1177	7646
B	4590	4293	6056
C	3304	3225	3333
D	11,180	10,680	32,549
E	23,027	24,386	107,367
F	2931	2931	7277
G	2005	2005	3825
Big pump base	1810	1810	5335
Small pump base	919	919	1726

as recommended by AWWA [12].

The pipelines that connect the pumps with the main pipelines have diameters D_e of 71 and 102 cm. The new pipeline starts with a diameter of 102 cm and ends at block E with a diameter of 234 cm.

3.4. *Thrust blocks geometry and properties*

The thrust blocks are made of reinforced concrete, a unit weight γ_c of 21.6 kN/m^3 was considered. They have different geometries, due to the pipes and fittings that must be fitted in the available space (Fig. 2). The blocks in the existing pipeline, F and G, have a slab foundation whereas the blocks in the new pipeline have shear keys to provide sliding and torsion resistance. Some acting forces are applied eccentrically which produce a torsional effect. The existing thrust blocks and the pump bases are shown in Fig. 6, their corresponding dimensions are in Table 1. The new thrust blocks are shown in Fig. 7.

Table 5
Elastic limit for translation and rotation of foundations.

Foundation	Elastic limit		
	Longitudinal displacement (m)	Transversal displacement (m)	Rotation (rad)
A	$1.53x10^{-04}$	$1.23x10^{-05}$	$2.47x10^{-04}$
B	$3.37x10^{-04}$	$8.68x10^{-05}$	$2.70x10^{-04}$
C	$2.90x10^{-04}$	$1.85x10^{-04}$	$4.23x10^{-04}$
D	$1.19x10^{-03}$	$6.41x10^{-05}$	$1.20x10^{-04}$
E	$8.36x10^{-05}$	$3.11x10^{-04}$	$3.06x10^{-04}$
F	$2.45x10^{-04}$	$1.90x10^{-05}$	$4.29x10^{-04}$
G	$1.12x10^{-04}$	$1.42x10^{-05}$	$6.26x10^{-04}$
Big pump base	$4.36x10^{-05}$	$1.22x10^{-05}$	$2.68x10^{-04}$
Small pump base	$8.08x10^{-05}$	$3.78x10^{-05}$	$5.30x10^{-04}$

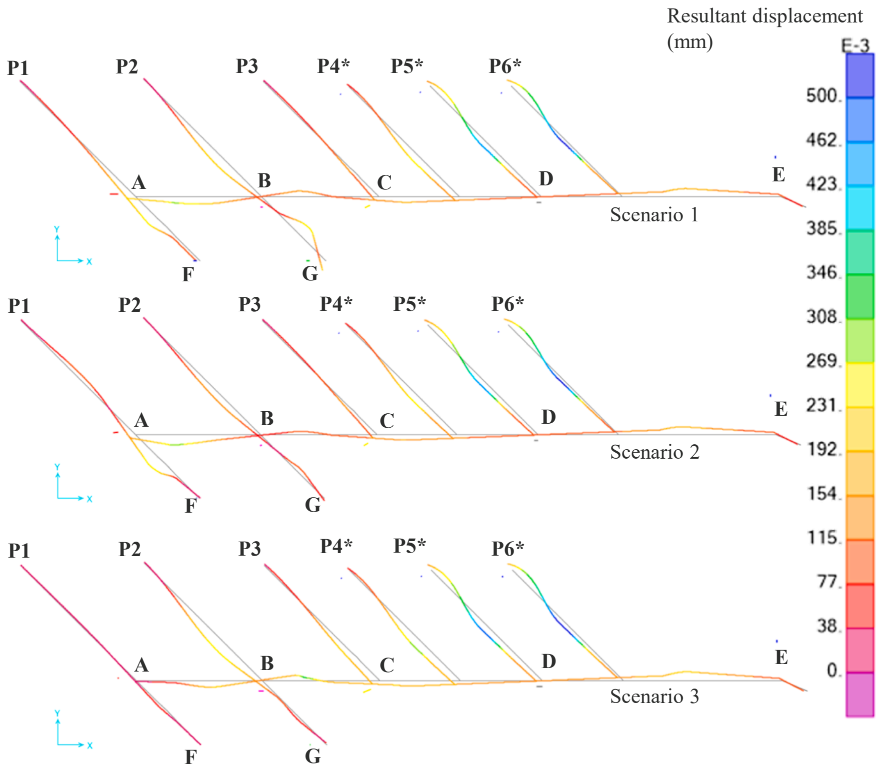

Fig. 12. Operating condition: resultant displacement for the three scenarios (scale factor × 5000).

3.5. Hydraulic pressures

In both pipelines, under normal operating conditions (PO), the maximum internal pressure is 2.1 MPa. In transient flow (PT), the maximum internal pressure is 2.9 MPa. With these pressures, the thrust forces were calculated according to AWWA [12]. The pump pipelines are connected to the main pipelines at an angle θ of 45°. The forces induced by the reducers and the operation of the valves are also included.

3.6. Scenarios of operation

The forces correspond to hydraulic actions in the pipe by pressure, geometry, and changes in diameter and direction. The three scenarios included are: 1) Simultaneous flow in both pipelines (Fig. 8a); 2) Flow in the new pipeline starting at block A, (pipeline 1 out of service, Fig. 8b); and 3) Flow in the new pipeline starting at block C (pipeline 1 out of service, Fig. 8c). Scenarios 1 and 2 are considered highly probable to occur; while the scenario 3 represents a possible adverse scenario for the manifolds, especially for the thrust block C. Forces (F) are indicated in normal operation and their position are depicted in Fig. 9 and Table 2. For the case of

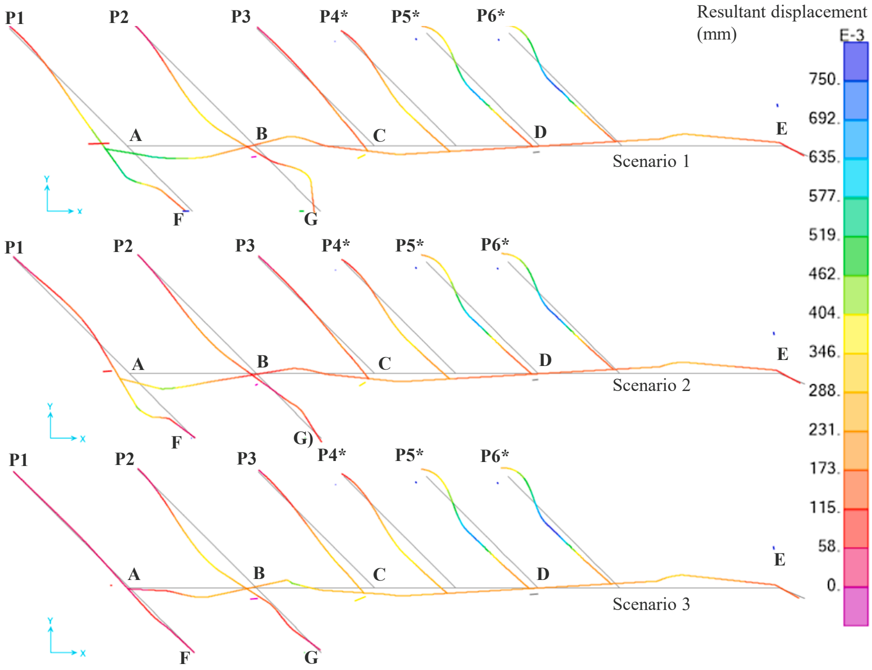

Fig. 13. Transient condition: resultant displacement for the three scenarios (scale factor × 5000).

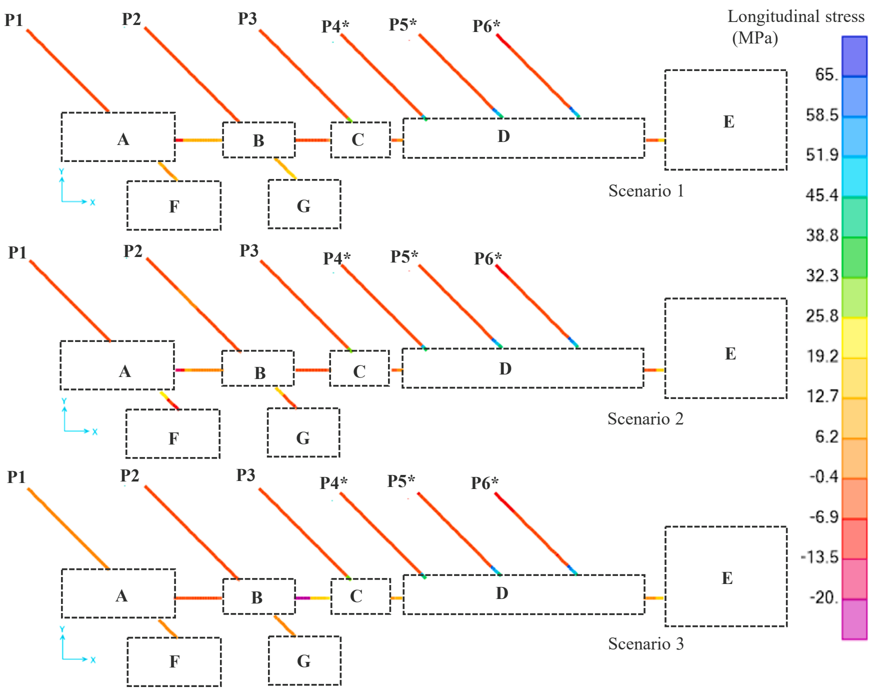

Fig. 14. Operating condition: longitudinal stress for the three scenarios.

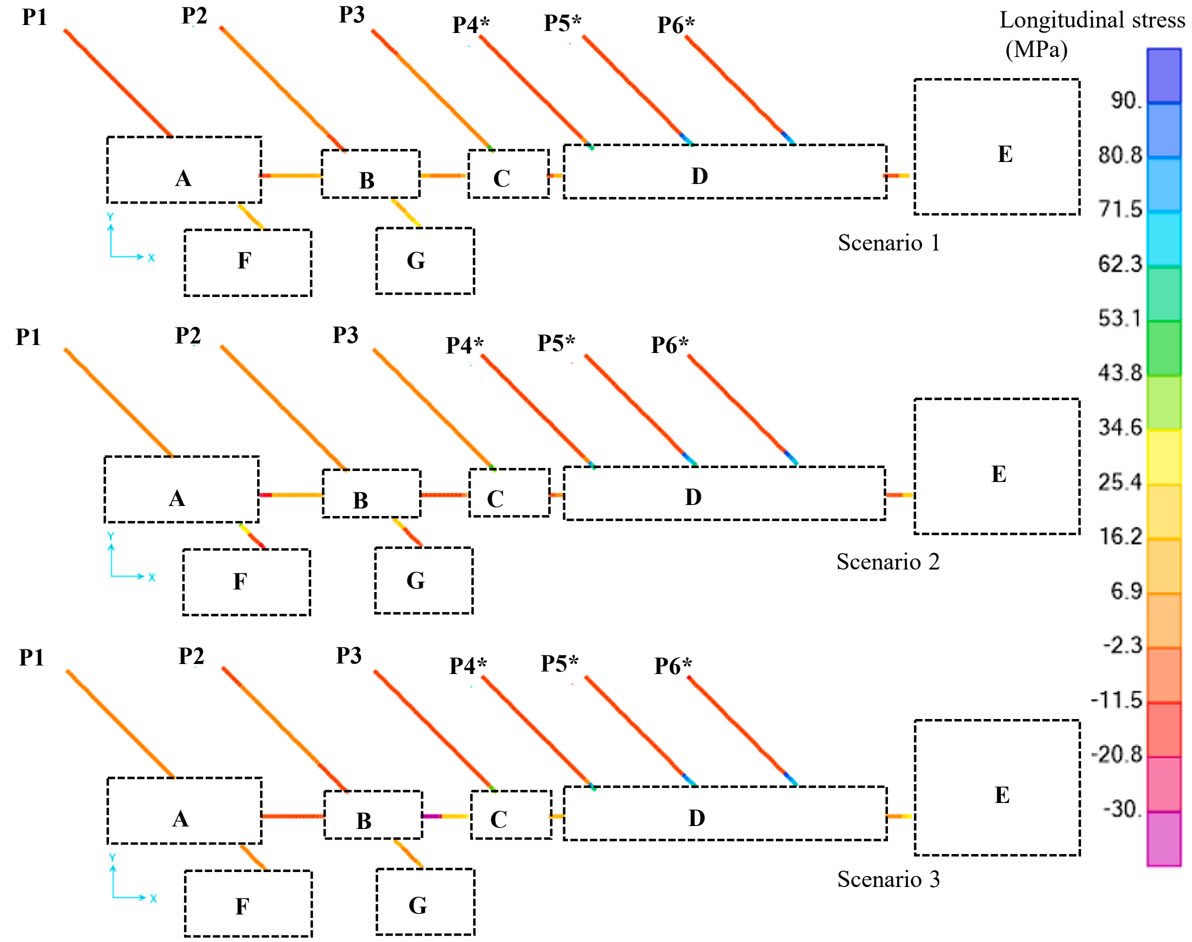

Fig. 15. Transient condition: longitudinal stress for the three scenarios.

transient flow, the forces determined in normal operation were multiplied by a factor of 1.43, which is the ratio between the transient pressure and the normal operating pressure (2.9/2.1 MPa).

4. Analysis and revision considerations to the case study

The process for analysis and revision of discharge manifolds used by the authors (Fig. 10) took into account the common design recommendations (Fig. 3 and Fig. 4). The enhanced method considers the additional effects. These effects are due to space restrictions that are not included in the common methodology. The additional effects considered are the soil-block-pipe interaction and the fittings not encased. These effects are presented in the operating and transient conditions. The redistribution of additional stresses in the manifold are calculated using the numerical model. In the revision, the effects considered in the common methodology were incorporated analytically to the additional ones.

For the foundation stability of the thrust blocks and pump bases, the sliding revision was performed. The safety factors considered for this revision are 1.5, for operating conditions; and 1.3, for transient conditions. Moreover, the authors included a torsional analysis. The proposed safety factors for this revision are 1.5, for operating conditions; and 1.2, for transient conditions. The torsional effect was calculated considering the shear flow between the soil and the foundation base and the distance between the resultant and the shear center.

The design considerations included the displacements of the thrust blocks and pump bases and the effects of the fittings not encased in the blocks into the pipeline; in such a way that, the combined stresses in the pipeline segments were calculated, including the additional longitudinal stresses.

5. Numerical model description

To estimate the additional effects due to soil-block-pipe interaction and the reducers outside the blocks in the revision, a numerical model of the discharge manifold is proposed. The aim of the model is to represent the displacement of the blocks and bases, and the

Table 6
Foundation reactions with structural interaction.

Foundation	Condition	Reaction forces								
		Case 1			Case 2			Case 3		
		L (kN)	T (kN)	T_z (kN-m)	L (kN)	T (kN)	T_z (kN-m)	L (kN)	T (kN)	T_z (kN-m)
A	PO	−1971	−192	−560	−1487	−721	−1078	−325	−38	−219
	PT	−1971	−600	−998	−1971	−1088	−1575	−464	−54	−313
B	PO	−798	−415	688	−453	−943	481	−1548	−315	676
	PT	−1436	−662	1145	−699	−1359	716	−2210	−450	965
C	PO	−1286	−1071	−127	−1192	−1104	−112	−2002	−1162	−70
	PT	−1912	−1509	−188	−1715	−1575	−161	−2860	−1660	−99
D	PO	−854	−1659	2237	−823	−1650	2163	−1185	−1531	2216
	PT	−1247	−2374	3240	−1180	−2358	3099	−1693	−2188	3166
E	PO	−2378	4582	−4356	−2349	4581	−4234	−2748	4514	−5148
	PT	−3425	6544	−6318	−3360	6544	−6066	−3926	6449	−7354
F	PO	−948	−955	18	214	−349	331	−30	7	79
	PT	−1660	−1110	277	251	−453	519	−43	9	113
G	PO	−1188	−755	−706	172	−213	−194	−132	184	131
	PT	−1724	−1040	−985	240	−297	−273	−189	263	188
P1	PO	−95	0	151	−29	2	59	−8	0	15
	PT	−239	−1	374	−61	2	113	−11	1	21
P2	PO	−43	−2	53	−20	−1	20	−74	−2	99
	PT	−76	−4	95	−30	−2	31	−105	−3	141
P3	PO	−104	0	166	−100	0	160	−144	−1	224
	PT	−152	0	243	−144	0	229	−206	−2	320
P4*	PO	−88	−1	107	−88	−1	106	−100	−1	121
	PT	−127	−2	153	−126	−2	152	−143	−2	173
P5*	PO	−230	−3	275	−229	−3	273	−243	−3	289
	PT	−330	−4	393	−327	−4	390	−347	−4	413
P6*	PO	−274	−3	336	−272	−3	333	−286	−3	351
	PT	−392	−4	482	−388	−4	477	−409	−5	501

PO: Operating pressure.
PT: Transient pressure.

stress distribution that develops along the pipe segments. The model considered a simplified approach to design purposes. Thus, a frame and spring model is proposed (Fig. 11). The interaction of the blocks and bases with the soil was modeled with a nonlinear spring with elasto-plastic behavior. The pipeline segments were modeled as linear elastic. The pipe was represented with second-order frame elements (two nodes). The pipeline segments embedded at the thrust blocks were considered rigid using a three-dimensional rigid body constraint.

The interaction between the foundations (thrust blocks and pump bases) and the soil was represented by spring elements (two nodes). Springs were placed at the shear centers of the foundations (Fig. 11) to take into account the torsional moments. The local axes of the spring elements are depicted as green (longitudinal) and blue (transversal) arrows, respectively. The vertical displacement was neglected because most of it occurred during the construction of the thrust blocks. The out-of-plane effects were not considered, because the overturning resistance was not exceeded. The force–displacement (translational spring) and moment-rotation (rotational spring) laws were considered as elastoplastic with perfect plasticity behavior. The maximum sliding and torsional resistance are determined by the yielding. Thus, when these resistances are reached, the thrust blocks and pump bases slide or rotate freely; restricted only by the rigidity due to the pipeline segments and the adjacent blocks or bases. In the foundation resistance, the soil passive reaction was not considered as explained in Section 2.2.

The rigidity of the translational spring k_s was determined by the modulus of horizontal stiffness of the foundation (blocks or bases), estimated by equation (1) [17]:

$$k_s = \overline{k}_{s1}\frac{n+0.5}{1.5n} \tag{1}$$

where n is the ratio L/B between the length L and the width B of the contact area of the foundation. The contact area is the perpendicular area to the direction of the expected force and displacement. $\overline{k_{s1}}$ is the average unit modulus of the foundation, which can be evaluated from the results of the plate load test. A $\overline{k_{s1}}$ value of 236,831 kN/m^3 was considered.

The rotational stiffness k_ψ for the spring was defined by the modulus of rotational stiffness of the foundation, calculated by equation (2) [18]:

$$k_\psi = \frac{M_z}{\psi} = c_\psi J_z \tag{2}$$

where M_z is the rotational moment around the vertical axis (torsional moment), ψ is the angle of rotation, J_z is the polar moment of

Table 7
Foundation reactions without structural interaction.

Foundations	Condition	Reaction forces								
		Case 1			Case 2			Case 3		
		L (kN)	T (kN)	T_z (kN-m)	L (kN)	T (kN)	T_z (kN-m)	L (kN)	T (kN)	T_z (kN-m)
A	PO	−2824	0	−765	−1755	−1069	−2599	0	0	0
	PT	−4031	0	−1089	−2511	−1530	−3717	0	0	0
B	PO	−686	0	785	382	−1069	−1255	0	0	0
	PT	−981	0	1118	549	−1530	−1795	0	0	0
C	PO	−1451	−1069	696	−1451	−1069	696	−4962	−1069	2805
	PT	−2069	−1530	991	−2069	−1530	991	−7090	−1530	4001
D	PO	−2226	−1481	1903	−2226	−1481	1903	−2226	−1481	1903
	PT	−3177	−2118	2717	−3177	−2118	2717	−3177	−2118	2717
E	PO	−1393	4805	−2903	−1393	4805	−2903	−1393	4805	−2903
	PT	−1991	6865	−4148	−1991	6865	−4148	−1991	6865	−4148
F	PO	−726	−1069	−392	0	0	0	0	0	0
	PT	−1040	−1530	−559	0	0	0	0	0	0
G	PO	−716	−1069	−1952	0	0	0	0	0	0
	PT	−1020	−1530	−2785	0	0	0	0	0	0
P1	PO	0	0	0	0	0	0	0	0	0
	PT	0	0	0	0	0	0	0	0	0
P2	PO	0	0	0	0	0	0	0	0	0
	PT	0	0	0	0	0	0	0	0	0
P3	PO	0	0	0	0	0	0	0	0	0
	PT	0	0	0	0	0	0	0	0	0
P4*	PO	0	0	0	0	0	0	0	0	0
	PT	0	0	0	0	0	0	0	0	0
P5*	PO	0	0	0	0	0	0	0	0	0
	PT	0	0	0	0	0	0	0	0	0
P6*	PO	0	0	0	0	0	0	0	0	0
	PT	0	0	0	0	0	0	0	0	0

PO: Operating pressure.
PT: Transient pressure.

inertia of the contact area of the foundation and c_ψ is the coefficient of non-uniform elastic shear. Barkan [18] suggests c_ψ values depending on the type of material and the area of the foundation considered. A c_ψ value of 26.5 N/cm^3 was considered in this study.

The torsional stiffnesses are determined for each foundation (Table 3). The calculated resistances of the thrust blocks and pumps bases for sliding and rotation are summarized in Table 4. By considering the maximum sliding and torsional resistances, their elastic limits to displacement and rotation were defined, respectively (Table 5).

The three scenarios of operation (see Section 3.6) were represented by three load cases. The position of the calculated forces applied to the numerical model is shown in Fig. 9 and the values of these forces are shown in Table 2.

6. Structural behavior of the manifold

The deformed shapes of the three scenarios are compared in Fig. 12 and Fig. 13. The interaction produces relative displacements between the blocks and their bases. In the main pipeline, the displacement increases along the X-axis direction. This displacement is opposite to the water flow direction. Therefore, in each operating scenario, the block with the largest displacement is the first one in the water flow direction of the main pipeline: block A for scenarios 1 and 2, and block C for scenario 3. In scenarios 1 and 2, block A develops nonlinear behavior, its sliding resistance is exceeded in the longitudinal direction. The maximum displacements are present in scenario 1. These are 0.19 and 0.46 mm in operating and transient conditions, respectively. The deformed shapes show that the movements are transferred by the pipelines to the adjoining block or base. Additionally, in scenarios 2 and 3, a displacement develops in the parts with no operation of the manifold. For example, blocks F and A in the scenario 2 and 3, respectively. In contrast, the fittings not embedded in the blocks show a negligible effect on the deformed shapes.

The soil-block-pipeline interaction and the fittings not encased in the blocks produce longitudinal stresses in the pipeline segments (Fig. 14 and Fig. 15). In the pipeline segment between A and B, the interaction effects develop longitudinal stresses between −26 and 19 MPa for the operating condition and between −36 and 26 MPa for the transient condition. The longitudinal stress is produced by the relative displacement between blocks and bases. On the other hand, the fittings outside the blocks exhibit longitudinal stresses up to 65 and 97 MPa in operating and transient conditions. The maximum stresses are present in the pipeline segment between block D and its pump. In contrast, the shear stresses are insignificant (lower than 0.5 MPa). Since the block rotations are within the elastic range (Table 6).

The foundation reactions with and without interaction effects are compared in Tables 6 and 7. In the main pipeline, the reaction difference is between −63 and 97% for longitudinal force; between –33 and 12% for transversal force; and between −77 and 98% for torsional moment. In this comparison, the positive difference represents a reaction increment. In some cases, the torsional moment

Table 8
Load - resistance ratio of thrust blocks and pump bases with no interaction.

Block / Base	Condition	Applied load to capacity ratio								
		Scenario 1			Scenario 2			Scenario 3		
		L	T	T_z	L	T	T_z	L	T	T_z
A	PO	1.43	0.00	0.10	0.89	0.91	0.34	0.00	0.00	0.00
	PT	2.05	0.00	0.14	1.27	1.30	0.49	0.00	0.00	0.00
B	PO	0.15	0.00	0.13	0.08	0.25	0.21	0.00	0.00	0.00
	PT	0.21	0.00	0.18	0.12	0.36	0.30	0.00	0.00	0.00
C	PO	0.44	0.33	0.21	0.44	0.33	0.21	1.50	0.33	0.84
	PT	0.63	0.47	0.30	0.63	0.47	0.30	2.15	0.47	1.20
D	PO	0.20	0.14	0.06	0.20	0.14	0.06	0.20	0.14	0.06
	PT	0.28	0.20	0.08	0.28	0.20	0.08	0.28	0.20	0.08
E	PO	0.06	0.20	0.03	0.06	0.20	0.03	0.06	0.20	0.03
	PT	0.09	0.28	0.04	0.09	0.28	0.04	0.09	0.28	0.04
F	PO	0.25	0.36	0.05	0.00	0.00	0.00	0.00	0.00	0.00
	PT	0.35	0.52	0.08	0.00	0.00	0.00	0.00	0.00	0.00
G	PO	0.36	0.53	0.51	0.00	0.00	0.00	0.00	0.00	0.00
	PT	0.51	0.76	0.73	0.00	0.00	0.00	0.00	0.00	0.00
P1	PO	0	0	0	0	0	0	0	0	0
	PT	0	0	0	0	0	0	0	0	0
P2	PO	0	0	0	0	0	0	0	0	0
	PT	0	0	0	0	0	0	0	0	0
P3	PO	0	0	0	0	0	0	0	0	0
	PT	0	0	0	0	0	0	0	0	0
P4*	PO	0	0	0	0	0	0	0	0	0
	PT	0	0	0	0	0	0	0	0	0
P5*	PO	0	0	0	0	0	0	0	0	0
	PT	0	0	0	0	0	0	0	0	0
P6*	PO	0	0	0	0	0	0	0	0	0
	PT	0	0	0	0	0	0	0	0	0

PO: Operating pressure
PT: Transient pressure
Light grey cell: load exceeds limit recommended by common design
Dark grey cell: load reaches the structural resistance

changes its direction (block C). Furthermore, the pump bases present not only reactions at their foundation, but also induced forces by the interaction effects. These effects allow the load distributions by means of pipeline segments. The pipeline segments that connect bases with the blocks have a lower longitudinal stiffness than the others. The lower stiffness is due to its longer length compared to the pipeline segments between the blocks of the main pipeline (Fig. 2). Nevertheless, the P3 foundation presents reactions up to −409 kN and 501 kN-m in its longitudinal force and torsional moment, respectively.

The effects due to the soil-block-pipeline interaction allow the manifolds to behave as a structural system. The interaction influences the longitudinal stress of the pipeline and the deformed shapes and the foundation reactions of the blocks and bases. On the other hand, the fittings outside the blocks exhibit significant longitudinal stress. Both additional effects should be considered to analyze the structural behavior of the manifolds.

7. Comparison between the common and enhanced methods

7.1. Evaluation of blocks and bases

The analyses of blocks and bases were performed considering the interaction effects. The foundation reactions with and without interaction and the individual foundation capacities are compared. In the load-resistance and the displacement-elastic limit ratios, a value of 1 or more means that the individual capacity is exceeded. A value of 0.67 or more means that the recommended design limit for operating conditions in the common design is exceeded. For transient conditions, these design limit values are 0.77 and 0.83, for sliding and torsional revision, respectively. In this way, the limit ratios of 0.67, 0.77, 0.83 and 1 are equivalent to safety factors of 1.5, 1.3, 1.2 and 1, respectively. Additionally, in the case of load-resistance ratio of bases, the ratio is zero because the pump bases do not have any load applied directly. The displacement-elastic limit ratio cannot be calculated by the common method, because of the blocks

Table 9
Load - resistance ratio of thrust blocks and pump bases with interaction.

Block / Base	Condition	Applied load to capacity ratio								
		Scenario 1			Scenario 2			Scenario 3		
		L	T	T_z	L	T	T_z	L	T	T_z
A	PO	1.00	0.16	0.07	0.75	0.61	0.14	0.16	0.03	0.03
	PT	1.00	0.51	0.13	1.00	0.92	0.21	0.24	0.05	0.04
B	PO	0.17	0.10	0.11	0.10	0.22	0.08	0.34	0.07	0.11
	PT	0.31	0.15	0.19	0.15	0.32	0.12	0.48	0.10	0.16
C	PO	0.39	0.33	0.04	0.36	0.34	0.03	0.61	0.36	0.02
	PT	0.58	0.47	0.06	0.52	0.49	0.05	0.87	0.51	0.03
D	PO	0.08	0.16	0.07	0.07	0.15	0.07	0.11	0.14	0.07
	PT	0.11	0.22	0.10	0.11	0.22	0.10	0.15	0.20	0.10
E	PO	0.10	0.19	0.04	0.10	0.19	0.04	0.12	0.19	0.05
	PT	0.15	0.27	0.06	0.15	0.27	0.06	0.17	0.26	0.07
F	PO	0.32	0.33	0.00	0.07	0.12	0.05	0.01	0.00	0.01
	PT	0.57	0.38	0.04	0.09	0.15	0.07	0.01	0.00	0.02
G	PO	0.59	0.38	0.18	0.09	0.11	0.05	0.07	0.09	0.03
	PT	0.86	0.52	0.26	0.12	0.15	0.07	0.09	0.13	0.05
P1	PO	0.05	0.00	0.03	0.02	0.00	0.01	0.00	0.00	0.00
	PT	0.13	0.00	0.07	0.03	0.00	0.02	0.01	0.00	0.00
P2	PO	0.02	0.00	0.01	0.01	0.00	0.00	0.04	0.00	0.02
	PT	0.04	0.00	0.02	0.02	0.00	0.01	0.06	0.00	0.03
P3	PO	0.06	0.00	0.03	0.06	0.00	0.03	0.08	0.00	0.04
	PT	0.08	0.00	0.05	0.08	0.00	0.04	0.11	0.00	0.06
P4*	PO	0.10	0.00	0.06	0.10	0.00	0.06	0.11	0.00	0.07
	PT	0.14	0.00	0.09	0.14	0.00	0.09	0.16	0.00	0.10
P5*	PO	0.25	0.00	0.16	0.25	0.00	0.16	0.26	0.00	0.17
	PT	0.36	0.00	0.23	0.36	0.00	0.23	0.38	0.00	0.24
P6*	PO	0.30	0.00	0.19	0.30	0.00	0.19	0.31	0.00	0.20
	PT	0.43	0.00	0.28	0.42	0.00	0.28	0.45	0.01	0.29

PO: Operating pressure
PT: Transient pressure
Light grey cell: load exceeds limit recommended by common design
Dark grey cell: load reaches the structural resistance

and bases displacements are assumed as zero.

The load-resistance ratios for sliding and torsional bending of each block are compared in Tables 8 and 9. When it is considered the isolated behavior of each block, two blocks (A and C, light, and dark grey cells) exceed the design recommendations. Also, blocks A and C overpass their resistances (dark grey cells). In scenarios 1 and 2, block A exceeds its longitudinal sliding resistance up to 105% (in scenario 1). In scenario 3, block C overpasses its rotational moment resistance up to 120%. When the interaction is accounted for, the load is distributed according to the stiffness of the blocks, bases, and pipelines. This can be seen from the reduction in the load-resistance ratio of moment rotation due to the redistribution in the elastic range (Fig. 12, Fig. 13 and Table 10). In scenarios 1 and 2, block A develops nonlinear behavior because its sliding resistance in the longitudinal axis is reached. Nevertheless, its longitudinal displacement is less than 0.5 mm, 3 times its elastic limit (Table 10). This is due to the load transfer via the pipeline to the adjoining blocks (B and F) and base (P1). It can be noted from their sliding-resistance ratio increments.

When the soil-block-pipeline interaction is taken into account, the loads acting on the blocks and bases are different from those calculated using the common manual methodology. The load redistribution is present due to the elastic range behavior. Therefore, the foundation resistances are defined by the soil friction. These effects need to be considered to prevent an underestimation or over-estimation of design loads. Especially for the pump bases which do not have externally applied loads. In contrast, even though a block reaches its individual resistance, the manifold performs satisfactorily because of the interaction effects. Additionally, the torsional evaluation is not usually considered by the common recommendations. The design guidelines do not provide minimum safety factors for this case. However, as it was shown by the analysis, it can be of utmost importance if the forces are not applied near the shear center of the thrust block.

Table 10
Displacement – elastic limit ratio at thrust blocks and base pumps with interaction.

Block / Base	Condition	Displacement – Elastic limit ratio								
		Scenario 1			Scenario 2			Scenario 3		
		L	T	T_z	L	T	T_z	L	T	T_z
A	PO	1.23	0.16	0.07	0.75	0.61	0.14	0.16	0.03	0.03
	PT	2.97	0.51	0.13	1.29	0.90	0.21	0.23	0.05	0.04
B	PO	0.18	0.10	0.11	0.10	0.22	0.08	0.34	0.07	0.11
	PT	0.31	0.15	0.19	0.15	0.31	0.12	0.48	0.10	0.16
C	PO	0.39	0.33	0.04	0.36	0.34	0.03	0.61	0.36	0.02
	PT	0.58	0.47	0.06	0.52	0.49	0.05	0.86	0.51	0.03
D	PO	0.08	0.16	0.07	0.07	0.15	0.07	0.11	0.14	0.07
	PT	0.11	0.22	0.10	0.11	0.22	0.09	0.15	0.20	0.10
E	PO	0.10	0.19	0.04	0.10	0.19	0.04	0.12	0.19	0.05
	PT	0.14	0.27	0.06	0.14	0.27	0.06	0.17	0.26	0.07
F	PO	0.32	0.33	0.00	0.07	0.12	0.05	0.01	0.00	0.01
	PT	0.57	0.38	0.04	0.09	0.15	0.07	0.01	0.00	0.02
G	PO	0.59	0.38	0.19	0.09	0.11	0.05	0.07	0.09	0.04
	PT	0.85	0.52	0.26	0.12	0.15	0.07	0.10	0.13	0.05
P1	PO	0.05	0.00	0.03	0.02	0.00	0.01	0.00	0.00	0.00
	PT	0.13	0.00	0.07	0.03	0.00	0.02	0.01	0.00	0.00
P2	PO	0.02	0.00	0.01	0.01	0.00	0.00	0.04	0.00	0.02
	PT	0.04	0.00	0.02	0.02	0.00	0.01	0.06	0.00	0.03
P3	PO	0.06	0.00	0.03	0.06	0.00	0.03	0.08	0.00	0.04
	PT	0.08	0.00	0.04	0.08	0.00	0.04	0.11	0.00	0.06
P4*	PO	0.10	0.00	0.06	0.10	0.00	0.06	0.11	0.00	0.07
	PT	0.14	0.00	0.09	0.14	0.00	0.09	0.16	0.00	0.10
P5*	PO	0.25	0.00	0.16	0.25	0.00	0.16	0.26	0.00	0.17
	PT	0.36	0.00	0.23	0.36	0.00	0.23	0.37	0.00	0.24
P6*	PO	0.30	0.00	0.19	0.30	0.00	0.19	0.31	0.00	0.20
	PT	0.43	0.00	0.28	0.42	0.00	0.28	0.45	0.01	0.29

PO: Operating pressure
PT: Transient pressure
Light grey cell: displacement exceeds the recommendation by common design
Dark grey cell: load reaches the elastic limit

7.2. Evaluation of pipelines segments

The effects of the interaction and the fittings outside the blocks on the pipeline segments are evaluated. For this purpose, the maximum equivalent stresses due to the three operation scenarios were calculated. The considered stresses are (Table 11): i) self-weight (DL), ii) internal pressure (IP), iii) structural interaction (SI), and iv) fittings or special parts (SP). In this evaluation a negative sign means compression.

The maximum equivalent stresses of the pipeline segments are compared in Fig. 16. In this evaluation, negative and positive values indicate stress decreases and increases, respectively. These influences produce additional longitudinal stresses on pipeline segments. These stresses are unconsidered by the common analysis and design. The longitudinal stresses are between −25 and 67 MPa in operating conditions and between −36 and 95 MPa in transient conditions (Fig. 14 and Fig. 15). In the pipeline segments with fittings outside the blocks, the equivalent stresses are increased up to 47% by the conical transitions and by the valves 20%. In the pipe sections with no fittings, the equivalent stresses change is less than 10%. This is due to the relative movement between the blocks and the bases because of the soil-block-pipeline interaction.

The maximum equivalent stresses determined from the three load cases are evaluated with the allowable stresses for normal operating and transient conditions. Two evaluations are performed (Fig. 17). The first with the effects of the structural interaction and the fittings outside the blocks. The second without them. A value less than or equal to 1 means that the equivalent stress is lower than the allowable stress; thus, the pipe section is acceptable; otherwise, it is unacceptable. In all cases, the equivalent stress is lower than the allowable stress; therefore, the structural sections of pipe segments are suitable. The critical section (D-E) is defined by the internal

Table 11
Pipeline segment stresses (MPa).

Segment	Condition	Stresses					Combinations				
		σ_C IP	σ_L DL	σ_L IP	σ_L SI + SP		σ_C IP	σ_L IP + DL		σ_L DL + IP + SI + SP	
					min	max		min	max	min	max
P1 - A	PO	43.4	±3.0	13.0	−1.6	0.5	43.4	10.0	16.0	8.4	16.5
	PT	61.9	±3.0	18.6	−4.2	0.6	61.9	15.5	21.6	11.3	22.2
P2 - B	PO	43.4	±3.4	13.0	−2.1	0.5	43.4	9.6	16.4	7.5	16.9
	PT	61.9	±3.4	18.6	−3.0	0.7	61.9	15.2	22.0	12.2	22.7
P3 - C	PO	60.7	±3.0	18.2	−2.3	33.1	60.7	15.2	21.2	12.9	54.3
	PT	86.7	±3.0	26.0	−3.2	47.3	86.7	23.1	29.0	19.9	76.3
P4* - D	PO	58.5	±9.5	17.6	−2.8	54.6	58.5	8.0	27.1	5.2	81.7
	PT	83.6	±9.5	25.1	−4.0	78.0	83.6	15.5	34.6	11.5	112.6
P5* - D	PO	62.9	±9.5	18.9	−2.5	62.1	62.9	9.3	28.4	6.8	90.5
	PT	89.8	±9.5	26.9	−3.5	88.7	89.8	17.4	36.5	13.9	125.2
P6* - D	PO	65.0	±5.9	19.5	−2.8	66.0	65.0	13.6	25.4	10.8	91.4
	PT	92.9	±5.9	27.9	−4.0	94.4	92.9	22.0	33.8	18.0	128.2
A - B	PO	58.5	±2.8	17.6	−16.2	7.2	58.5	14.7	20.4	−1.5	27.6
	PT	83.6	±2.8	25.1	−22.1	15.6	83.6	22.2	27.9	0.1	43.5
B - A1	PO	65.0	±1.3	19.5	−25.1	20.3	65.0	18.2	20.8	−6.9	41.1
	PT	92.9	±1.3	27.9	−35.9	28.9	92.9	26.5	29.2	−9.4	58.1
B - C	PO	83.7	±0.1	25.1	−4.6	9.8	83.7	25.0	25.2	20.4	35.0
	PT	119.6	±0.1	35.9	−6.5	14.0	119.6	35.7	36.0	29.2	50.0
C - D	PO	110.7	±0.3	33.2	−3.3	18.2	110.7	32.9	33.6	29.6	51.8
	PT	158.1	±0.3	47.4	−4.6	26.0	158.1	47.1	47.8	42.5	73.8
A - E	PO	43.4	±0.3	13.0	−10.0	24.6	43.4	12.7	13.3	2.7	37.9
	PT	61.9	±0.3	18.6	−13.7	35.9	61.9	18.3	18.9	4.6	54.8
B - F	PO	43.4	±0.5	13.0	−7.2	19.7	43.4	12.5	13.5	5.3	33.2
	PT	61.9	±0.5	18.6	−10.1	28.2	61.9	18.1	19.0	8.0	47.2

PO: Operating pressure.
PT: Transient pressure.
σC: Circumferential stress.
σL: Longitudinal stress.

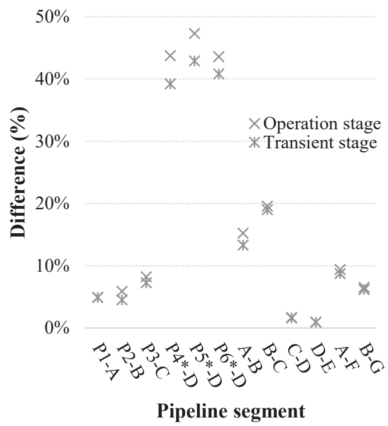

Fig. 16. Effect of the structural interaction and the fittings on equivalent stresses.

pressure.

From the results, it is concluded that the effects of structural interaction on the pipe segments are negligible. Between blocks A and B, approximately 1260 kN can be transferred by the sliding of the block A. In the segment that connects them (A-B), this load transfer changes the equivalent stress less than 15%. This produces a longitudinal stress less than 16 MPa in the pipe ($D_e = 1.37$ m and $t^{'} = 24.23$ mm). In contrast, fittings not encased in the blocks cause significant stress increases. A conical transition can increase the equivalent stress up to 47%. Nevertheless, the allowable stress was not exceeded. Thus, both effects do not compromise the security and the operation of a manifold.

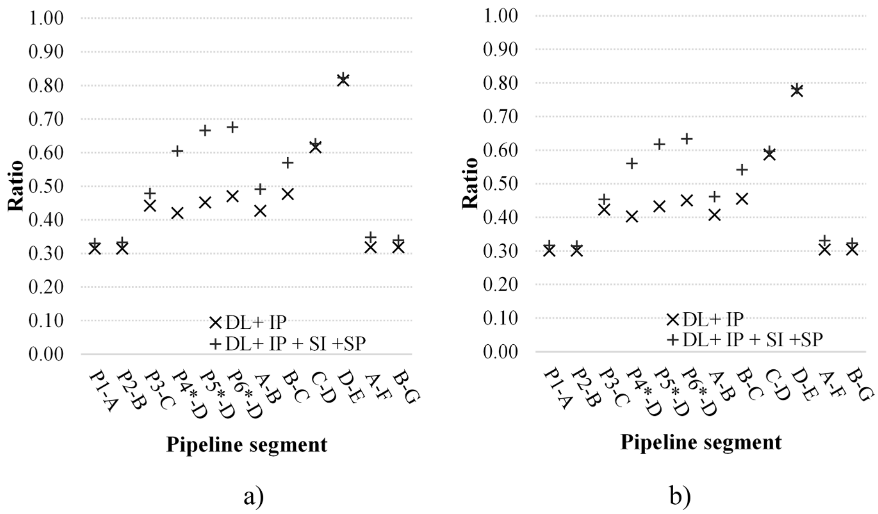

Fig. 17. Comparison between equivalent and allowable stresses: a) operating condition; b) transient condition.

8. Conclusions

Due to the space restrictions, the modification of discharge manifolds can lead to nonconventional arrangements. These arrangements can be fittings to lie close to each other and not encased in the thrust blocks. The space restrictions also limit the size of the thrust blocks. These conditions produce an effect of soil-block-pipeline interaction in the manifolds. Also, the fittings not encased increase the stresses in the pipe segments. Both effects are not considered by the common methods for the analysis and design of supported pipelines. Therefore, in these cases, the enhanced method proposed is suitable.

From the results of the study case, it is concluded that the effects were significant on the manifold behavior. In the blocks, the soil-block-pipeline interaction produces forces and displacements that begin with load application. This effect changes the mechanical elements. The block forces increased up to 98% than the ones calculated by the current design practice. Despite one block presents sliding, its displacement was lower than 0.5 mm. The movements were transferred by the pipelines to the adjoining block or base. In the pipe segments, the main effect is in the longitudinal axis. The stresses change less than 10% the equivalent stress, which can be considered as negligible. Also, the shear stresses were insignificant (lower than 1 MPa) due to the block rotation in the elastic range. On the other hand, the fittings not encased in the blocks produced significant longitudinal stresses. The equivalent stresses increased up to 47% in the conical transitions. In the valves, the increase was 20%. These effects are quite important. Thus, the additional effects must be considered in the revision of the manifold. In this way, the proposed model that represents the manifold was essential. The numerical model incorporates the additional effects and the force redistribution between the manifold elements. On the other hand, the evaluation of the manifold with the space restrictions determined that block A reached its sliding resistance. Also, significant increments of equivalent stresses were determined in fittings not encased within the thrust block. Based on the results of this work, the manifold structure was suitable for operation.

Finally, the main advantage of the upgraded methodology is the consideration of additional effects by means of the proposed model. The upgrade incorporates the effects due to the soil-thrust blocks-pipeline interaction and the fittings outside the blocks. To include these, the model must represent the manifold behavior as a whole. Additionally, the torsional evaluation was included. Thus, the proposed method is suitable for the analysis, revision, and design of new and old discharge manifolds that have space restrictions.

Declaration of Competing Interest

The authors declare that they have no known competing financial interests or personal relationships that could have appeared to influence the work reported in this paper.

Acknoweledgement

The second author acknowledges the Postdoctoral grant by “Instituto de Ingeniería of the Universidad Nacional Autónoma de México” (IIUNAM).

References

[1] K.R. Bushdiecker, J.M. Ross, M.D. Gossett, Between a Track and a Hard Place - Thrust Restraint Alternatives in a Constrained Location, Pipelines 2018: Condition Assessment, Construction, and Rehabilitation, American Society of Civil Engineers, Toronto, Ontario, 2018, 10.1061/9780784481646.017.

[2] J.K. Jeyapalan, S.K. Rajah, Lessons from the Failure of Two Reclaimed Water Lines in California, Pipelines, 2007: Advances and Experiences with Trenchless Pipeline Projects, American Society of Civil Engineers, Boston, Massachusetts, 2007, 10.1061/40934(252)56.
[3] E. Kuliczkowska, A. Kuliczkowski, B. Tchórzewska-Cieślak, The structural integrity of water pipelines by considering the different loads, Eng. Fail. Anal. 118 (2020), 104932, https://doi.org/10.1016/j.engfailanal.2020.104932.
[4] K. Pietrucha-Urbanik, Failure analysis and assessment on the exemplary water supply network, Eng. Fail. Anal. 57 (2015), https://doi.org/10.1016/j.engfailanal.2015.07.036.
[5] ASCE, Manuals and Reports on Engineering Practice No. 79: Steel Penstocks, American Society of Civil Engineers, Reston, Virginia, 2012, 10.1061/9780784412169.
[6] Mapas, 6, Manual de agua potable, alcantarillado y saneamiento: estudios técnicos para proyectos de agua potable, alcantarillado y saneamiento: diseño estructural (in Spanish), Comisión Nacional del Agua, Ciudad de México (2015).
[7] ASCE Task Committee on Thrust Restraint Design of Buried Pipelines, Contribution of Frictional Resistance to Restrain Unbalanced Thrust in Buried Pipelines, Pipelines 2010: Climbing New Peaks to Infrastructure Reliability—Renew, Rehab, and Reinvest, American Society of Civil Engineers, Keystone, Colorado, 2010, 10.1061/41138(386)29.
[8] Subcommittee on Continuous Pipelines and ASCE Task Committee on Thrust Restraint Design of Buried Pipelines, An Improved Approach for the Design of Thrust Blocks in Buried Pipelines, Pipelines 2011: A Sound Conduit for Sharing Solutions, American Society of Civil Engineers, Seattle, Washington, 2011, 10.1061/41187(420)76.
[9] S.K. Rajah, J.K. Jeyapalan, W.E. Saleira, M.W. McCabe, R. Grodt, Soil Structure Interaction Effects in Thrust Restraint Systems of Buried Pipelines, Pipelines 2004 International Conference, American Society of Civil Engineers, San Diego, California, 2004, 10.1061/40745(146)21.
[10] L. Zhang, X. Yan, X. Yang, Using the Unit Force Method to Analyze Thrust Acting on Anchor Blocks Caused by Thermal Expansion Displacement of X80 Tunnel Pipelines, J. Pipeline Syst. Eng. Pract. 7 (1) (2016) 04015012, https://doi.org/10.1061/(ASCE)PS.1949-1204.0000202.
[11] H. H. Bardakjian, M. S. Zarghamee, Design of a 120 in.-Diameter Steel Bifurcation with a Small Acute Angle for a High-Pressure Penstock, Pipelines Congress 2008, American Society of Civil Engineers, Atlanta, Georgia, 2008, 10.1061/40994(321)30.
[12] American Water Works Association (AWWA), Manual of Water Supply Practices M11 Steel Pipe-A Guide for Design and Installation, 5th Edition, American Water Works Association, Denver, Colorado, 2018.
[13] A.R. Thorley, J. Atkinson, CIRIA Report 128: Guide to the design of thrust blocks for buried pressure pipelines, Construction Industry Research and Information Association, London, 1994.
[14] S.A. Karamanos, G.C. Sarvanis, B.D. Keil, R.J. Card, Analysis and Design of Buried Steel Water Pipelines in Seismic Areas, J. Pipeline Syst. Eng. Pract 8 (4) (2017) 04017018, https://doi.org/10.1061/(ASCE)PS.1949-1204.0000280.
[15] L.M. Matta, R. Dotson, Analysis of unburied pipeline spans, American Society of Mechanical Engineers, Calgary, Alberta, 2012, 10.1115/IPC2012-90579.
[16] K. Terzaghi, R. Peck, Soil Mechanics in Engineering Practice, John Wiley, New York, 1967.
[17] L. Zeevaert, Foundation Engineering for Difficult Subsoil Conditions, Van Nostrand Reinhold, New York, 1982.
[18] D. Barkan, Dynamics of Bases and Foundations, McGraw-Hill Inc., USA, 1962.